

# Anelastic Behavior under Tensile and Shearing Stresses in Bulk Metallic Glasses

Kazutaka Fujita<sup>1</sup>, Akihisa Inoue<sup>2</sup>, Tao Zhang<sup>2</sup> and Nobuyuki Nishiyama<sup>3</sup>

<sup>1</sup>Department of Mechanical Engineering, Ube National College of Technology Ube 755-8555, Japan

<sup>2</sup>Institute for Materials Research, Tohoku University, Sendai 980-8577, Japan

<sup>3</sup>Inoue Superliquid Glass Project, Exploratory Research for Advanced Technology, Japan Science and Technology Corporation, Sendai 982-0807, Japan

It is known that an anelastic deformation occurs more remarkably for amorphous ribbon alloys than for crystalline metallic alloys by the tensile test. In addition, the result of the molecular dynamics simulation on tensile and shearing tests for Cu single component amorphous metal has indicated that the anelastic deformation occurs more remarkably under the shearing stress rather than under the tensile stress. In this report, tensile and torsional tests were actually performed for bulk metallic glasses to examine the difference in the anelastic behavior under shearing and tensile stresses. Single-phase bulk metallic glasses,  $\text{La}_{60}\text{Al}_{20}\text{Ni}_{10}\text{Cu}_5\text{Co}_5$ ,  $\text{Pd}_{40}\text{Cu}_{30}\text{Ni}_{10}\text{P}_{20}$  and  $\text{Zr}_{55}\text{Cu}_{30}\text{Ni}_5\text{Al}_{10}$  (at%), were chosen together with a steel, JIS SGD 400-D, as a representative of metallic crystals. The test specimens were a round bar shape and the diameters of a parallel gage section were 4 to 10 mm. No anelastic behavior was observed for the steel under tensile and shearing stresses. Although the metallic glasses did not exhibit distinct anelastic deformation under the tensile stress, the shearing stress mode leads to a significant anelastic deformation even at low stress level. The amount of the anelastic deformation increases with an increase in the shearing stress level.

(Received March 20, 2002; Accepted May 16, 2002)

**Keywords:** anelasticity, bulk metallic glass, tensile stress, shearing stress, torsion

## 1. Introduction

Metallic glasses have high strength and low elastic modulus in comparison with metallic crystals.<sup>1)</sup> For metallic glasses the tensile and compressive fractures and the fatigue crack growth in the medium growth rate range occur along the maximum shearing stress plane declined to the loading axis even for bulk samples,<sup>2-4)</sup> while for metallic crystals they occur along the plane perpendicular to the loading axis.<sup>5)</sup> An anelastic deformation by tensile test occurs more remarkably for amorphous alloy sheets than for metallic crystals.<sup>6)</sup> As mentioned above, mechanical properties such as elastic deformation and fracture behavior for metallic glasses are significantly different from those for metallic crystals. In addition, one of the authors has simulated tensile and shearing tests for Cu single component amorphous metal using the molecular dynamics method, and reported that the anelastic behavior occurs more remarkably under the shearing stress than under the tensile stress.<sup>7)</sup> In this report, tensile and torsional tests were actually carried out for some bulk metallic glasses to clarify the anelastic behavior of metallic glasses under the shearing and tensile stresses.

## 2. Experimental Procedure

Bulk metallic glasses with compositions of  $\text{La}_{60}\text{Al}_{20}\text{Ni}_{10}\text{Cu}_5\text{Co}_5$ ,  $\text{Pd}_{40}\text{Cu}_{30}\text{Ni}_{10}\text{P}_{20}$  and  $\text{Zr}_{55}\text{Cu}_{30}\text{Ni}_5\text{Al}_{10}$  (at%) were examined. A commercial steel, JIS SGD 400-D, was also used as a representative of metallic crystals for comparison. Figure 1 shows the shape and dimension of the test specimens. The diameter in the parallel gage section was 4 to 6 mm for tensile test, (a), 5.5 mm for torsional rupture test, (b), and 10 mm for torsional test within an elastic limit, (c). An electro-hydraulic servo controlled testing machine for axial force and displacement (Shimadzu, EHF-U 50kN)

was used for both torsional and tensile tests. Figure 2 shows the photographs of the torsional testing apparatus. The torsional test was performed using a jig which converts a linear displacement of the piston-rod to the angular displacement. Continuously it was transmitted to the test specimen through a torsion-bar. The piston-rod displacement rate was fixed at  $0.01 \text{ mm} \cdot \text{s}^{-1}$  (the angular velocity = approximately  $1 \times 10^{-4} \text{ rad} \cdot \text{s}^{-1}$ ; shearing strain rate = approximately  $1.1 \times 10^{-5} \text{ s}^{-1}$ ) in all torsional tests. The torque was calculated from the strain measured by strain gages stuck on the torsion bar, and the angle of twist was obtained from the angular displacement between the plates for gripping specimen measured by a clip-gage. The relationship between the angle of twist and angular displacement was decided by the preliminary test. The tensile test was performed under the load control mode, and the stress-loading rate was fixed at almost the same value as the shearing stress loading rate. The tensile stress ( $\sigma$ ) and strain ( $\epsilon$ ) were measured with the load cell and the clip-gage of the 12.5 mm in gage length, respectively.

## 3. Results and Discussion

### 3.1 Torsional rupture test

Torsional rupture tests were made for the Pd-based bulk metallic glass and steel. Figure 3 shows the relationship between the torque ( $T$ ) and angle of twist ( $\phi$ ). The shearing stress ( $\tau$ ) and strain ( $\gamma$ ) were obtained by the common equation of elasticity, i.e.,  $\tau = 16T/(\pi d^3)$  and  $\gamma = \phi(d/2)/l$ , respectively. The  $d$  and  $l$  are the diameter and length of the parallel gage section, respectively. The values of  $\tau$  and  $\gamma$  are the ones on the surface in the parallel gage section of the specimens caused by all torsional tests. For the Pd-based metallic glass (Fig. 3(a)), since no yielding phenomenon was observed, the shearing strength  $\tau_B$  in the torsional test was also estimated by the above equation using the rupture torque

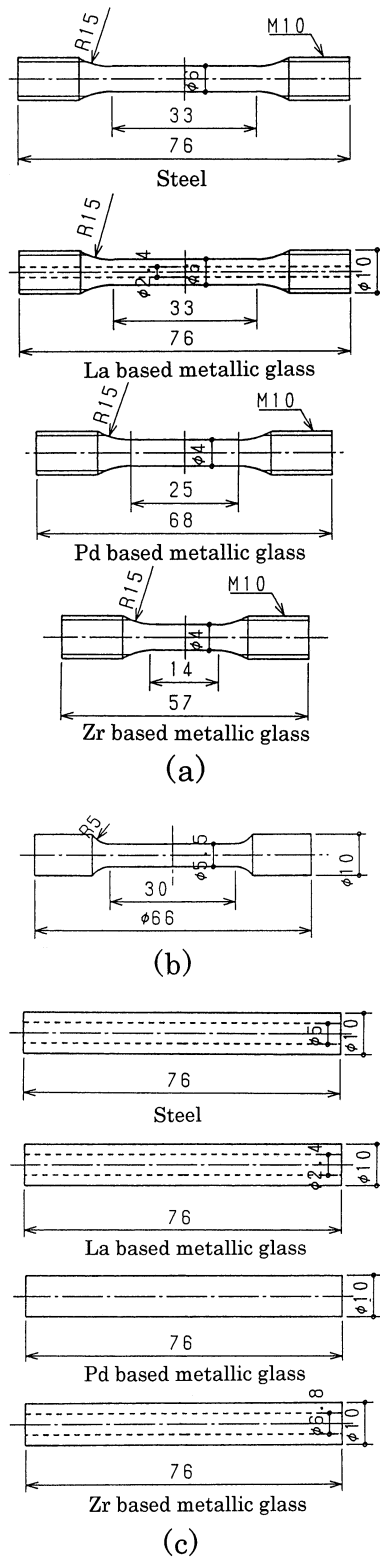


Fig. 1 Shape and dimensions of the test specimens for (a) tensile, (b) torsional rupture and (c) torsional tests.

( $T_B$ ). The value of  $\tau_B$  was 980 MPa. The tensile strength  $\sigma_B$  of the Pd-based metallic glass in literature<sup>1)</sup> is 1640 MPa and it nearly agrees with the value, 1700 MPa, estimated from the value of  $\tau_B$  using the relation of the equivalent stress of Mises  $\sigma = \sqrt{3} \cdot \tau$ .<sup>8)</sup> From this result, the values of  $\tau_B$  for the La- and Zr-based bulk metallic glasses were also estimated from the values of  $\sigma_B$  in literature<sup>1)</sup> using the relation of Mises.

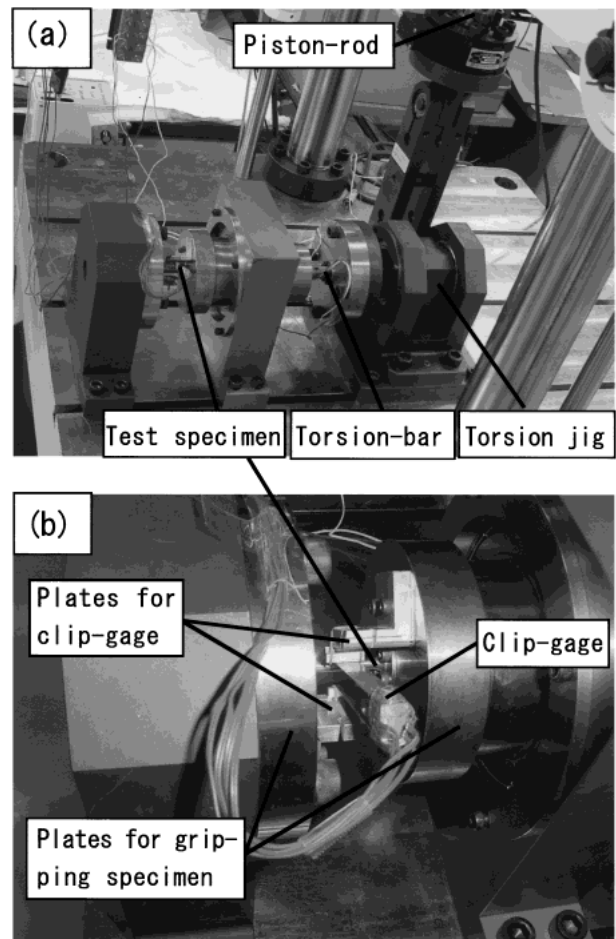


Fig. 2 The torsional testing apparatus. (a) General view and (b) enlarged view near a specimen.

Table 1 Chemical composition and mechanical properties of test materials.

Materials (at%)	$E$ (GPa)	$G$ (GPa)	$\sigma_B$ (MPa)	$\tau_B$ (MPa)
Steel (JIS SGD400-D)	200	80	660*	380
La <sub>60</sub> Al <sub>20</sub> Ni <sub>10</sub> Cu <sub>5</sub> Co <sub>5</sub>	38	12	1000 <sup>1)</sup>	580*
Pd <sub>40</sub> Cu <sub>30</sub> Ni <sub>10</sub> P <sub>20</sub>	94	32	1640 <sup>1)</sup>	980
Zr <sub>55</sub> Cu <sub>30</sub> Ni <sub>5</sub> Al <sub>10</sub>	85	31	1800 <sup>1)</sup>	1040*

$E$  = Young's modulus;  $G$  = Shear modulus;  $\sigma_B$  = Tensile strength;  $\tau_B$  = Shearing strength; \* = Estimated value

In the steel (Fig. 3(b)) with a distinct yielding phenomenon, the  $\tau_B$  in the torsional test was estimated by the equation,  $\tau_B = 12T_B/(\pi d^3)$ ,<sup>9)</sup> which was required under the assumption of general yield for rigid-perfectly plastic body. The value of  $\sigma_B$  was decided as the mean value of the standard  $\sigma_B$  range of this steel. These  $\sigma_B$  and  $\tau_B$  values are shown in Table 1. The following tensile and torsional tests were carried out under the test conditions decided on the basis of these  $\sigma_B$  and  $\tau_B$  values.

### 3.2 Tensile and torsional tests

Figures 4 and 5 show loading and unloading stress-strain curves for the steel and the metallic glasses, respectively. Each maximum stress was fixed as an approximately 30% of the fracture strength. For the steel, the loading  $\sigma$ - $\epsilon$  curve agrees well with the unloading one, and the loading  $\tau$ - $\gamma$  curve

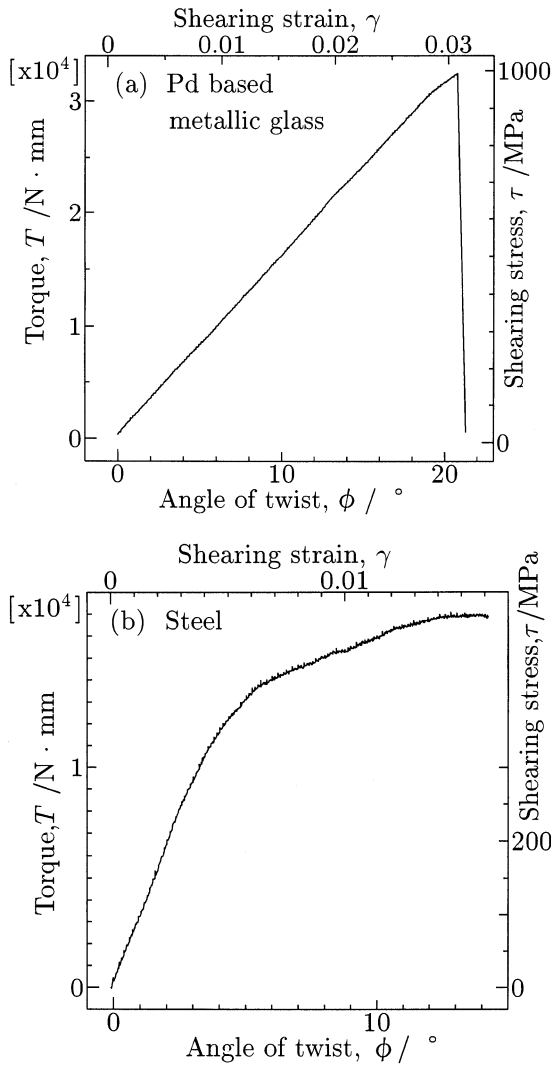


Fig. 3 Relationship between the torque and angle of twist in torsional rupture tests for (a) the Pd-based bulk metallic glass and (b) conventional steel (JIS SGD 400-D).

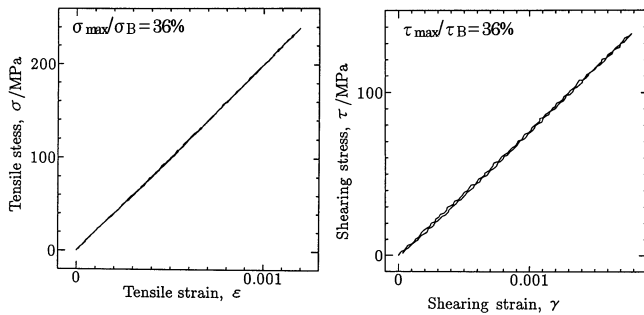


Fig. 4 Loading and unloading stress-strain curves in tensile and torsional tests for the steel. The ratios of maximum applied tensile stress/tensile strength ( $\sigma_{\max}/\sigma_B$ ) and maximum applied shearing stress/shearing strength ( $\tau_{\max}/\tau_B$ ) are fixed as an approximately 0.3.

is also in agreement with the unloading one, as shown in Fig. 4. For the La-based metallic glass, one can see an appreciable difference between loading and unloading  $\sigma$ - $\epsilon$  curves in the tensile test, while their curves of the Pd- and Zr-based metallic glasses do not have any difference and no anelastic phenomenon is observed. However, the loading and unloading  $\tau$ - $\gamma$  curves in the torsional tests do not agree distinctly for

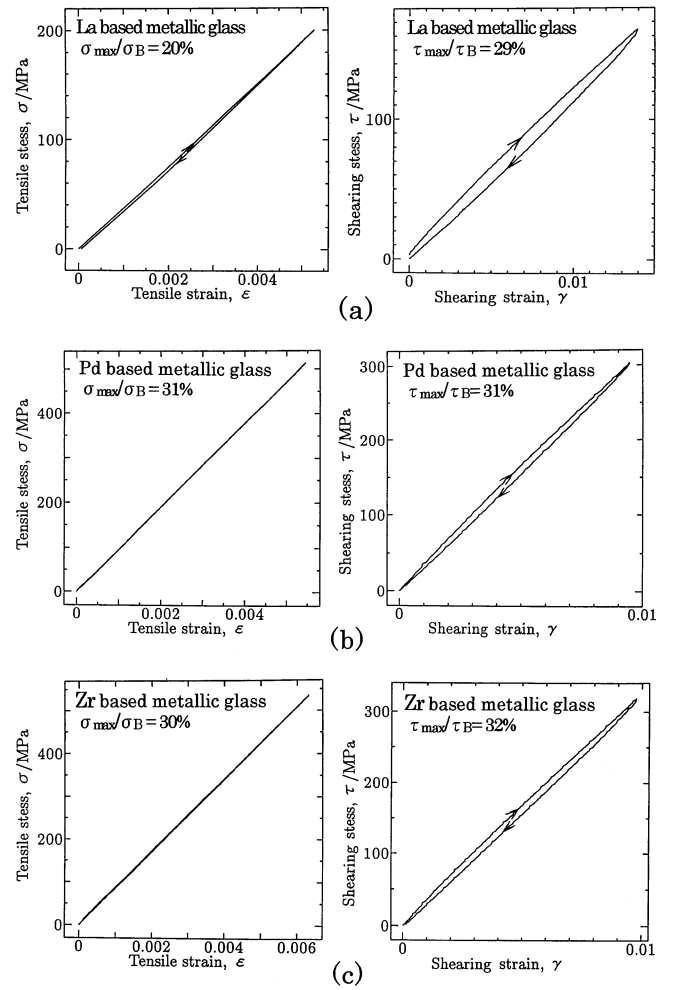


Fig. 5 Loading and unloading stress-strain curves in tensile and torsional tests for (a) the La-, (b) Pd- and (c) Zr-based bulk metallic glasses. The ratios of  $\sigma_{\max}/\sigma_B$  and  $\tau_{\max}/\tau_B$  are approximately 0.3.

all the metallic glasses, indicating the generation of anelastic phenomena as shown in Fig. 5. Figure 6 shows the  $\sigma$ - $\epsilon$  curves at different stress levels in the tensile test for the Zr-based metallic glass. The loading curve agrees with the unloading one, even if the maximum stress values are changed in the range of 20 to 50% of the  $\sigma_B$  value. Figure 7 shows the  $\tau$ - $\gamma$  curves at different stress levels in the torsional test for the La-based metallic glass. An anelasticity is recognized even when the maximum stress value is as small as 4% of the  $\tau_B$  value. This tends to increase with an increase in the applied stress. The above-described result also agrees with the simulation result. The following results for the metallic glasses are known. That is, the fractures by tensile and compressive rupture tests occur along the maximum shearing stress plane which is declined by about 45 degrees to the direction of applied load,<sup>2)</sup> and the fatigue crack growth also occurs easily to one maximum shearing stress direction in the intermediate crack growth rate range in which the growth rate is almost proportional to the square of the stress intensity factor range.<sup>3,4)</sup> On the other hand, for the metallic crystal these fractures usually occur along the plane perpendicular to the loading axis. Although the reason for the generation of distinct anelastic phenomenon for metallic glasses under the shearing stress conditions remains unclear, its phenomenon

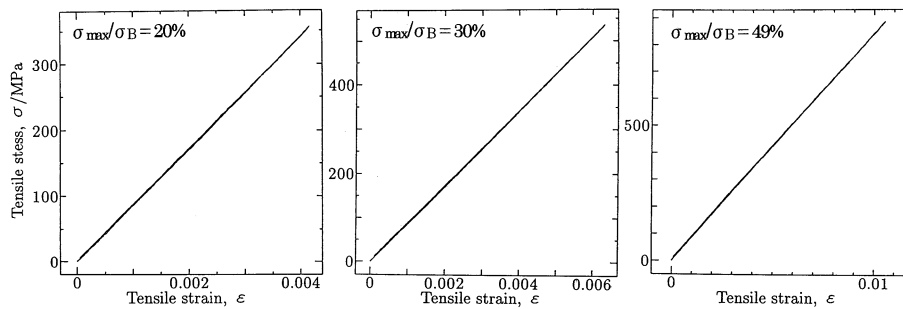


Fig. 6 Tensile loading and unloading stress-strain curves at different maximum stress levels for the Zr-based bulk metallic glass.

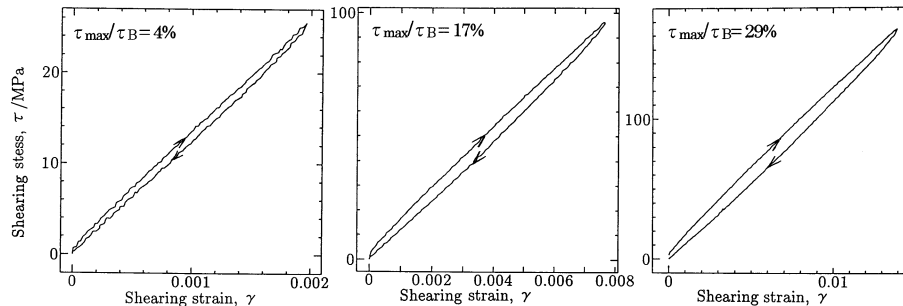


Fig. 7 Shear loading and unloading stress-strain curves at different maximum stress levels for the La-based bulk metallic glass.

may be similar to the destruction of the metallic glass related to the maximum shearing stress and shearing deformation. It is subsequently necessary to examine in more details the appropriateness of this mechanism through molecular dynamics simulations.

#### 4. Conclusions

The deformation behavior under tensile and torsional applied loads was examined for the La-, Pd- and Zr-based bulk metallic glasses, in comparison with the steel as a representative of metallic crystals. No anelastic phenomenon under tensile and shearing stresses was observed for the steel. The metallic glasses do not exhibit a distinct anelastic phenomenon under the tensile stress, but the application of shearing stress causes the appearance of anelastic phenomenon even at low stress levels and the anelasticity increases with an increase in the shearing stress.

#### Acknowledgements

This work was supported by the inter-university cooperative research program of the Institute for Materials Research, Tohoku University.

#### REFERENCES

- 1) A. Inoue: *Bulk Amorphous Alloys*, (Trans Tech Publications, Zurich, 1998).
- 2) T. Murata, T. Masumoto and M. Sakai: *Proc. 3rd Int. Conf. Rapidly Quenched Metals, II* (1980) 401.
- 3) K. Fujita, A. Inoue and T. Zhang: *Mater. Trans., JIM* **41** (2000) 1448–1453.
- 4) K. Fujita, A. Inoue and T. Zhang: *Scr. Mater.* **44** (2001) 1629–1633.
- 5) R. Koterazawa: *Strength and Fracture of Materials*, (Asakura, Tokyo, 1985) p. 70, p. 142.
- 6) T. Masumoto: *Sci. Rep. RITU A-26* (1977) 1625.
- 7) K. Fujita and M. Watanabe: *Proc. of Jpn. Soc. Mech. Eng.* **995-1** (1999) 47–48.
- 8) R. von Mises: *Göttinger Nachrichten, math.-phys. Klasse*, (1913) p. 582.
- 9) Y. Kawata, Y. Matsuura, M. Mizuno and M. Miyakawa: *Materials Test*, (Kyoritsu Shuppan, Tokyo, 1997) pp. 61–72.